AIAA JOURNAL
Vol. 31, No. 1, January 1993

Finite Element Nonlinear Panel Flutter with Arbitrary Temperatures in Supersonic Flow

David Y. Xue* and Chuh Mei†
Old Dominion University, Norfolk, Virginia 23529

A finite element frequency domain method for predicting nonlinear flutter response of panels with temperature effects is presented. From the principle of virtual work, the element nonlinear stiffness formulation for a panel under combined thermal and aerodynamic loads is derived, considering von Kármán's large deflection plate theory, the first-order piston theory aerodynamics, and quasisteady thermal stress theory. The system equations of motion can be mathematically separated into two sets of equations and solved sequentially. The first set of equations yields the panel thermal-aerodynamic equilibrium, and the second set of equations of motion leads to the flutter limit-cycle oscillations. They can be used to determine stability and flutter boundaries. Finite element large-amplitude limit-cycle flutter results at different uniform temperatures are obtained for a simply supported square panel and are compared with existing Galerkin/time integration and other finite element solutions. Effects of nonuniform temperature distributions, panel length-to-width ratios, and boundary conditions on flutter responses of rectangular and triangular panels are presented.

Nomenclature

$[A]$, $[D]$	= in-plane and bending stiffness matrices
$[a_a]$, $[A_a]$	= element and system aerodynamic influence matrices
a, b, h	= plate length, width, and thickness
c	= maximum limit-cycle amplitude
D	= bending rigidity, $Eh^3/12(1-\nu^2)$
$\{e\}$	= membrane strain vector
g_a	= nondimensional aerodynamic damping
$[k]$, $[K]$	= element and system stiffness matrices
M_∞	= Mach number (freestream)
$\{M\}$, $\{N\}$	= moment and force resultant vectors
$[m]$, $[M]$	= element and system mass matrices
$[n1]$, $[n2]$, $[N1]$, $[N2]$, $[K1]$, $[K2]$	= element and system nonlinear stiffness matrices
p_a	= aerodynamic pressure loading
$\{p\}$, $\{P\}$	= element and system forces
u, v, w	= element displacement functions
$\{w\}$, $\{W\}$	= element and system nodal displacements
x, y, z	= coordinate axes
α	= panel damping rate or coefficient of thermal expansion
ΔT	= temperature
$\{\epsilon\}$, $\{\sigma\}$	= total strain and stress vectors
$\{\kappa\}$, κ	= curvature, eigenvalue
λ	= nondimensional dynamic pressure, $2qa^3/D\sqrt{M_\infty^2-1}$
$\{\Phi\}$	= mode shape
Ω	= complex panel motion parameter, $\alpha + i\omega$
ω	= frequency

Subscripts

b	= bending
cr	= critical
l	= limit cycle, linear
m	= membrane
nl	= nonlinear
s	= static
t	= time dependent

Received March 19, 1992; presented as Paper 92-2129 at the AIAA Dynamics Specialists Conference, Dallas, TX, April 16-17, 1992; revision received July 7, 1992; accepted for publication July 7, 1992.

*Postdoctoral Fellow, Department of Mechanical Engineering and Mechanics. Member AIAA.

†Professor, Department of Mechanical Engineering and Mechanics. Associate Fellow AIAA.

Introduction

PANEL flutter is a self-excited oscillation of a plate in supersonic flow. Panel flutter differs from wing flutter only in that the aerodynamic force resulting from the airflow acts only on one side of the panel. In the framework of small deflection linear structural theory, there is a critical speed of the airflow (or dynamic pressure λ_{cr}) beyond which the panel motion becomes unstable and grows exponentially with time. Linear theory determines the critical dynamic pressure, frequency of vibration, and mode shape at the instability but usually gives no direct information about the panel deflection and stresses. Thus, the fatigue life of the panel cannot be predicted. A great quantity of literature exists on linear panel flutter using different aerodynamic theories, for example, Refs. 1 and 2, and many others. In reality, the panel not only bends but also stretches due to vibrations with large amplitude. Such membrane tensile forces in the panel provide a limited stabilizing effect that restrains the panel motion to bounded-amplitude limit-cycle oscillations, and the amplitude increases as the dynamic pressure increases. The external panel of a flight vehicle thus can withstand velocities beyond the critical value. Application of the nonlinear structural theory, which takes into account the induced membrane forces due to large deflections, yields not only the limit-cycle oscillating frequency but also panel deflections and stresses. With the maximum cyclic stress obtained together with the stress cycles to failure (S-N curve) material data, panel fatigue life can thus be estimated.[3] Two excellent surveys on nonlinear and linear panel flutter are given by Dowell[4] and, most recently, by Reed et al.[5]

The aerodynamic theory employed for the most part, and also for the present study, for panel flutter at high supersonic Mach numbers[2] ($M_\infty > 1.6$) is a quasisteady first-order piston theory aerodynamics.[6] The theory calculates the aerodynamic loads on the panel from local pressures generated by the body's motion as related to the local normal component of the fluid velocity. The primary aerodynamic force is proportional to the local panel slope. The other force, which is the aerodynamic damping force, is proportional to the transverse panel

velocity. Hence, the damping force is usually combined with the inertial force to yield an effective inertial force.

A number of classical analytic methods exist for the investigation of limit-cycle oscillations of panels in supersonic flow. In general, Galerkin's method is used in the spatial domain, where the panel deflection is expressed in terms of two to six or more linear normal modes; and various techniques in the temporal domain such as the numerical integration,[7-9] harmonic balance,[10-12] and perturbation[12,13] methods, to cite a few, are employed. All of the analytical investigations have been limited to two- or three-dimensional rectangular plates with all four edges simply supported or clamped. The classic approaches also indicated that at least six linear normal modes are required for a converged limit-cycle amplitude.

Application of the finite element method to study linear panel flutter was due to Olson.[14] Because of its versatile applicability, effects of general temperature distribution, aerodynamic damping, complex panel configuration (for example, delta planform[14]), airflow angularity, in-plane prestress, and laminated composite materials can be easily included. Extensions of the finite element methods to study supersonic/hypersonic limit-cycle oscillation of two-dimensional isotropic panels were given by Mei,[15] Rao and Rao,[16] Sarma and Varadan,[17] and Gray et al.[18]; three-dimensional isotropic panels by Mei and Weidman,[19] Mei and Wang,[20] and Han and Yang[21]; and laminated composite panels by Dixon and Mei[22] and Liaw and Yang.[23]

In most of the classic and finite element nonlinear panel flutter studies, the effects of uniform temperature change are treated by an equivalent system of mechanical loads. Few linear panel flutter studies have dealt with temperature distributions directly.[24-27] Because of the resurgent interest in flight vehicles, such as the High-Speed Civil Transport and the National Aero-Space Plane, the thermal effects due to nonuniform temperature distribution on limit-cycle motions of panels of complex configuration need to be addressed. Xue and Mei[3] have extended the finite element method to investigate the nonlinear flutter responses of two-dimensional panels with temperature distribution $\Delta T(x)$. The thermal environment can affect panel motions by introducing thermal in-plane forces and bending moments. Although mechanical loading can simulate and substitute for some simple temperature distributions, thermal stress analysis is necessary since simple mechanical loading cannot be substituted for complex temperature distribution.

This paper presents a consistent finite element formulation for analysis of large amplitude limit-cycle oscillations of panels of general planform with the influence of nonuniform temperature distribution $\Delta T(x, y, z)$. The von Kármán large-deflection plate theory is used to account for large thermal-aerodynamic deflections and large-amplitude limit-cycle oscillations, the quasisteady first-order piston theory is employed for aerodynamic loading, and the quasisteady thermal stress theory is applied for the thermal effects with a given temperature distribution. The finite element system differential equation of motion contains a time-independent thermal load vector. The total panel motion is thus the sum of a time-independent static equilibrium (particular) solution and a time-dependent self-excited dynamic (homogeneous) oscillation. The system equation of motion is then separated into two sets, static equilibrium and dynamic equations. They are nonlinear and coupled due to the simultaneously applied aerodynamic and thermal loads. The static equilibrium solution gives the thermal deflection of the panel with the influence of dynamic pressure, and it also yields the stability boundaries that distinguish panel behavior into flat panel, buckled panel, harmonic motion, and chaotic (snap-through) motion. Conversely, the solution from the set of dynamic equations of motion gives the large-amplitude limit-cycle flutter responses and dynamic (or flutter) stability boundaries. The present finite element formulation and the solution procedures are believed to be the first to study nonlinear flutter of panels of complex configuration with general temperature distribution. The modeling of complex configuration of panel planforms is accomplished by the use and the development of nonlinear stiffness and aerodynamic influence coefficient matrices for a discrete Kirchhoff theory (DKT) triangular plate element.[28-30] Finite element large-amplitude panel flutter results with uniform temperature distribution are compared with existing numerical time integration[9] and other finite element limit-cycle results. Effects of different temperature distributions, panel length-to-width ratios, and boundary conditions on nonlinear flutter responses and stability boundaries of rectangular and triangular panels are investigated.

Finite Element Formulation

The von Kármán strain-displacement relation for a general plate element undergoing both extension and bending at any point z through the thickness is the sum of membrane and change of curvature strain components as

$$\begin{Bmatrix} \epsilon_x \\ \epsilon_y \\ \gamma_{xy} \end{Bmatrix} = \{e\} + z\{\kappa\}$$

$$= \begin{Bmatrix} u_{,x} \\ v_{,y} \\ u_{,y} + v_{,x} \end{Bmatrix} + \frac{1}{2} \begin{Bmatrix} w_{,x}^2 \\ w_{,y}^2 \\ 2w_{,x}w_{,y} \end{Bmatrix} + z \begin{Bmatrix} -w_{,xx} \\ -w_{,yy} \\ -2w_{,xy} \end{Bmatrix} \tag{1}$$

For an isotropic elastic thin plate subjected to a temperature variation $\Delta T(x, y, z)$, the stress-strain relation is given by

$$\{\sigma\} = \begin{Bmatrix} \sigma_x \\ \sigma_y \\ \tau_{xy} \end{Bmatrix} = [E] \begin{Bmatrix} \epsilon_x \\ \epsilon_y \\ \gamma_{xy} \end{Bmatrix} - \frac{E\alpha\Delta T}{1-\nu} \begin{Bmatrix} 1 \\ 1 \\ 0 \end{Bmatrix} \tag{2}$$

where $[E]$ is the material stiffness matrix given next, α is the thermal expansion coefficient, and ν is the Poisson's ratio:

$$[E] = \frac{E}{1-\nu^2} \begin{bmatrix} 1 & \nu & 0 \\ \nu & 1 & 0 \\ 0 & 0 & \frac{1}{2}(1-\nu) \end{bmatrix} \tag{3}$$

The force and moment resultants are defined as

$$\{N, M\} = \int_{-h/2}^{h/2} (1, z)\{\sigma\}\, dz \tag{4}$$

which leads to

$$\{N\} = [A]\{e\} - \{N_{\Delta T}\} \tag{5}$$

$$\{M\} = [D]\{\kappa\} - \{M_{\Delta T}\} \tag{6}$$

where $[A] = h[E]$ and $[D] = (h^3/12)[E]$ are the in-plane and bending stiffness matrices; $\{N_{\Delta T}\}$ and $\{M_{\Delta T}\}$ are the thermal force and thermal moment vectors.

The first-order piston theory aerodynamics[4,6] is given by

$$p_a = -\frac{2q}{\sqrt{M_\infty^2 - 1}} \left(w_{,x} + \frac{M_\infty^2 - 2}{M_\infty^2 - 1} \frac{1}{V} w_{,t} \right)$$

$$= -\left(\lambda \frac{D}{a^3} w_{,x} + \frac{g_a}{\omega_0} \frac{D}{a^4} w_{,t} \right) \tag{7}$$

where $q = \rho_a V^2/2$ is the dynamic pressure, ρ_a the air density, V the airflow speed, M_∞ the Mach number, a the panel length, $D = Eh^3/12(1-\nu^2)$ the bending rigidity, and $\omega_0 = (D/\rho h a^4)^{1/2}$ a convenient reference frequency, and the nondimensional

dynamic pressure and aerodynamic damping coefficients are given by

$$\lambda = \frac{2qa^3}{D\sqrt{M_\infty^2 - 1}}, \qquad g_a = \frac{\rho_a V(M_\infty^2 - 2)}{\rho h \omega_0 (M_\infty^2 - 1)^{3/2}} \tag{8}$$

The principle of virtual work for a structure in equilibrium states that

$$\delta W = \delta W_{\text{int}} - \delta W_{\text{ext}} = 0 \tag{9}$$

where

$$\delta W_{\text{int}} = \int_A (\{\delta e\}^t \{N\} + \{\delta \kappa\}^t \{M\})\, dA \tag{10}$$

$$\delta W_{\text{ext}} = \int_A \delta w(-\rho h \ddot{w} + p_a)\, dA \tag{11}$$

and where ρ, h, and A are the mass density, thickness, and area of the plate element, respectively. With the application of virtual work and the use of finite element expression, the equations of motion for a plate element subjected to a temperature change $\Delta T(x, y, z)$ and dynamic pressure λ simultaneously can be written as

$$\frac{1}{\omega_0^2}\begin{bmatrix} m_b & 0 \\ 0 & 0 \end{bmatrix}\begin{Bmatrix} \ddot{w}_b \\ \ddot{w}_m \end{Bmatrix} + \frac{g_a}{\omega_0}\begin{bmatrix} g & 0 \\ 0 & 0 \end{bmatrix}\begin{Bmatrix} \dot{w}_b \\ \dot{w}_m \end{Bmatrix} + \left(\lambda\begin{bmatrix} a_a & 0 \\ 0 & 0 \end{bmatrix} + \begin{bmatrix} k_b - k_{N\Delta T} & 0 \\ 0 & k_m \end{bmatrix} + \frac{1}{2}\begin{bmatrix} n1_{Nm} & n1_{bm} \\ n1_{mb} & 0 \end{bmatrix} + \frac{1}{3}\begin{bmatrix} n2 & 0 \\ 0 & 0 \end{bmatrix}\right)\begin{Bmatrix} w_b \\ w_m \end{Bmatrix} = \begin{Bmatrix} p_{b\Delta T} \\ p_{m\Delta T} \end{Bmatrix} + \{f\} \tag{12}$$

where $\{w_b\}$ and $\{w_m\}$ are the element nodal bending and membrane displacement vectors; $[m]$, $[g]$, $[a_a]$, and $[k]$ are the element mass, aerodynamic damping, aerodynamic influence, and linear stiffness matrices, respectively; $[k_{N\Delta T}]$ is the geometric stiffness due to thermal forces; $[n1]$ and $[n2]$ are the nonlinear stiffness matrices that depend linearly and quadratically on element displacements, respectively; and $\{p_{\Delta T}\}$ and $\{f\}$ are the element thermal load and internal equilibrium force vectors. All element matrices are symmetrical except the aerodynamic influence matrix $[a_a]$, which is skew symmetric. The detailed derivation of the equation of motion, Eq. (12), is given in Ref. 31.

System Equations and Solution Procedures

By summing up the contributions from all of the elements and taking account of the kinematic boundary conditions, the system equations of motion for a given panel of general planform subjected to a combined temperature and airflow can be written in the matrix form as

$$\frac{1}{\omega_0^2}[M]\{\ddot{W}\} + \frac{g_a}{\omega_0}[G]\{\dot{W}\} + (\lambda[A_a] + [K] - [K_{N\Delta T}] + \tfrac{1}{2}[N1] + \tfrac{1}{3}[N2])\{W\} = \{P_{\Delta T}\} \tag{13}$$

Equation (13) is a set of nonlinear ordinary differential equations with respect to time t. The coupling of the airflow and temperature is shown by the presence of the $[G]$, $[A_a]$, and $[K_{N\Delta T}]$ matrices and the thermal load vector $\{P_{\Delta T}\}$. The solution procedure presented in the following is innovative for determining large-amplitude limit-cycle flutter response and stability boundaries from Eq. (13).

Preliminary Process

In Eq. (13), the force vector $\{P_{\Delta T}\}$ is independent of time t. The solution of a differential equation with a constant term, Eq. (13), is thus the sum of a time-dependent homogeneous solution and a time-independent particular solution, that is,

$$\{W\} = \{W\}_s + \{W(t)\}_t \tag{14}$$

where $\{W\}_t$ is the time-dependent homogeneous solution whose physical meaning is the self-excited dynamic oscillations, whereas $\{W\}_s$ is the particular solution whose physical meaning is the thermal-aerodynamic static equilibrium deflection.

Substituting Eq. (14) into the system equations of motion, Eq. (13), the following two sets of equations are obtained[3,31]:

$$(\lambda[A_a] + [K] - [K_{N\Delta T}] + \tfrac{1}{2}[N1]_s + \tfrac{1}{3}[N2]_s)\{W\}_s = \{P_{\Delta T}\} \tag{15}$$

$$\frac{1}{\omega_0^2}[M]\{\ddot{W}\}_t + \frac{g_a}{\omega_0}[G]\{\dot{W}\}_t + (\lambda[A_a] + [K] - [K_{N\Delta T}] + [N1]_s + [N2]_s)\{W\}_t + ([N2]_{st} + \tfrac{1}{2}[N1]_t + \tfrac{1}{3}[N2]_t)\{W\}_t = 0 \tag{16}$$

where the subscripts s and t to the system nonlinear stiffness matrices denote that the corresponding matrix is evaluated with $\{W\}_s$ or $\{W\}_t$. A close examination of Eqs. (15) and (16) reveals the following:

1) Equation (15) is a set of nonlinear algebraic equations that yields the thermal-aerodynamic deflection $\{W\}_s$.

2) Equation (16) is a set of nonlinear differential homogeneous (self-excited) equations that yields the limit-cycle motion $\{W\}_t$.

3) The two equations are coupled between the aerodynamic pressure ($\lambda[A_a]$ and $g_a[G]$) and temperature load ($\{P_{\Delta T}\}$ and $[K_{N\Delta T}]$).

4) Equation (15) has to be solved first to obtain $\{W\}_s$; then $\{W\}_t$ can be determined from Eq. (16).

Thermal-Aerodynamic Deflection

Equation (15) can be referred to as a thermal structural problem with the influence of dynamic pressure λ. First the critical bucking temperature is determined. The equations for the linear thermal buckling are obtained by neglecting the thermal bending moment, the nonlinear, and the aerodynamic terms from Eqs. (12) or (15) and they become[3,27,31]

$$[K_m]\{W_m\}_s = \{P_{m\Delta T}\} \tag{17}$$

$$[K_b]\{\Delta W_b\}_s = \mu([K_{N\Delta T}] - [N1_{Nm}]_s)\{\Delta W_b\}_s \tag{18}$$

The critical temperature is thus given by $\Delta T_{\text{cr}}(x, y, z) = \mu_1 \Delta T(x, y, z)$, where μ_1 is the lowest eigenvalue from Eq. (18).

For a given combination of dynamic pressure λ and temperature ratio $\Delta T(x, y, z)/\Delta T_{\text{cr}} > 1$, the thermal aerodynamic postbuckling deflection can be determined from Eq. (15) by using the well-known Newton-Raphson iteration method; that is, at the ith iteration[3,27,31]

$$[K_{\tan}]_i\{\Delta W_i\}_s = \{\Delta P\}_i \tag{19}$$

where the tangent stiffness matrix and the error vector are

$$[K_{\tan}]_i = \lambda[A_a] + [K] - [K_{N\Delta T}] + [N1_i]_s + [N2_i]_s \tag{20}$$

$$\{\Delta P\}_i = \{P_{\Delta T}\} - (\lambda[A_a] + [K] - [K_{N\Delta T}] + \tfrac{1}{2}[N1_i]_s + \tfrac{1}{3}[N2_i]_s)\{W_i\}_s \tag{21}$$

The converged postbuckling deflection is updated by $\{\Delta W_i\}_s$ as

$$\{W_{i+1}\}_s = \{W_i\}_s + \{\Delta W_i\}_s \tag{22}$$

until $\{\Delta P\}_i$ or $\{\Delta W_i\}_s$ approaches zero. There are three possible solutions from Eq. (15) with the various combinations of $\Delta T/\Delta T_{\text{cr}}$ and λ. They are 1) a buckled equilibrium position that corresponds to $\{W\}_s \neq 0$, 2) a flat equilibrium that corresponds to $\{W\}_s = 0$, and 3) the fact that the solution $\{W\}_s$ cannot be determined, which refers to a snap-through unstable status of the panel.[8,31]

Reduced System Dynamic Equation

The in-plane inertia is being neglected in the formulation in Eq. (12). Thus, the in-plane displacements, Eq. (16), can be expressed in terms of bending displacements as

$$\{W_m\}_t = -[K_m]^{-1}([N1_{mb}]_s + \tfrac{1}{2}[N1_{mb}]_t)\{W_b\}_t \tag{23}$$

and the dynamic equation, Eq. (16), leads to the reduced system equation which is expressed in terms of the transverse displacements $\{W_b\}_t$ only as

$$\frac{1}{\omega_0^2}[M_b]\{\ddot{W}_b\}_t + \frac{g_a}{\omega_0}[G]\{\dot{W}_b\}_t + ([K]_l + [K1]_{nl} + [K2]_{nl})\{W_b\}_t = 0 \tag{24}$$

where the linear and nonlinear stiffness matrices are

$$[K]_l = \lambda[A_a] + [K_b] - [K_{N\Delta T}] + [N1_{Nm}]_s + [N2]_s - [N1_{bm}]_s[K_m]^{-1}[N1_{mb}]_s \tag{25}$$

$$[K1]_{nl} = [N2]_{st} - [N1_{bm}]_t[K_m]^{-1}[N1_{mb}]_s - [N1_{bm}]_s[K_m]^{-1}\tfrac{1}{2}[N1_{mb}]_t \tag{26}$$

$$[K2]_{nl} = \tfrac{1}{3}[N2]_t - \tfrac{1}{2}[N1_{bm}]_t[K_m]^{-1}[N1_{mb}]_t \tag{27}$$

and where $[K1]_{nl}$ and $[K2]_{nl}$ depend linearly and quadratically on $\{W_b\}_t$, respectively. The matrices $[N1_{Nm}]_s$, $[N2]_s$, $[N1_{bm}]_s$, and $[N1_{mb}]_s$ in Eqs. (25) and (26) are known since $\{W\}_s$ has been determined from Eq. (15).

Critical Dynamic Pressure

By dropping the nonlinear terms in Eq. (24), the solution of the eigenvalue problem is of the form

$$\{W_b\}_t = \{\Phi_b\}e^{\Omega t} \tag{28}$$

where $\Omega = \alpha + i\omega$ is the complex panel motion parameter, and α and ω are the panel damping rate and frequency, respectively. It results in the following nondimensional eigenvalue equation:

$$\kappa[M_b]\{\Phi_b\} = [K]_l\{\Phi_b\} \tag{29}$$

where the nondimensional eigenvalue is

$$\kappa = -\left(\frac{\Omega}{\omega_0}\right)^2 - g_a\frac{\Omega}{\omega_0} \tag{30}$$

The eigenvalue includes the damping coefficient so that the aerodynamic damping matrix is absorbed into the mass matrix. This is possible since $[m_b] = [g]$.[3,14] The critical dynamic pressure is determined when the two lowest eigenvalues κ_1 and κ_2 coalesce to a value of κ_{cr}.[14,27]

Limit-Cycle Oscillations

In Eq. (24), the terms $[K1]_{nl}\{W_b\}_t$ and $[K2]_{nl}\{W_b\}_t$ contribute quadratic and cubic nonlinearities to the nonlinear equations. It is known that a nonlinear dynamic system with quadratic nonlinearity may have nonharmonic motions, whereas a nonlinear dynamic system with only cubic nonlinearity can have harmonic motions. Examining Eq. (26), note that all three terms of $[K1]_{nl}$ are depending on $\{W\}_s$, and also recall that three solutions are possible for the thermal-aerodynamic deflections from the static equation. Therefore, a flat thermal-aerodynamic deflection ($\{W\}_s = 0$) would lead to $[K1]_{nl} = 0$ and a limit-cycle harmonic motion for the dynamic response from Eq. (24), whereas a thermal-aerodynamically buckled panel ($\{W\}_s \neq 0$ and $[K1]_{nl} \neq 0$) leads to a nonharmonic periodic oscillation; when $\{W\}_s$ cannot be determined, the dynamic system results in chaotic or snap-through behavior. This further demonstrates the coupling of the static equilibrium and the dynamic equations, Eqs. (15) and (16). The static thermal-aerodynamic deflection solution will have great influence on the panel dynamic behavior.

The linearized updated mode with a nonlinear time function approximation (LUM/NTF) method is employed here in obtaining the limit-cycle flutter motions from Eq. (24). This LUM/NTF approach has been used successfully in the investigation of large-amplitude free and forced vibrations of laminated composite plates[32] and nonlinear panel flutter.[3,18,22,31] The solution to the homogeneous dynamic equation is sought in the form of

$$\{W_b\}_t = \bar{c}\{\Phi_b\}e^{\Omega t} \tag{31}$$

where $\bar{c}$ is a nonzero (scalar) constant displacement amplitude and $\{\Phi_b\}$ is generally a complex eigenvector. Recognizing that, in developing the system equation, all of the system quantities used are real, it must be concluded that the nodal response quantities must also be real.[2] These nodal quantities can be approximated by taking only the real part of the normalized Eq. (31) as

$$\{W_b\}_t = \frac{\bar{c}e^{\alpha t}}{|(\Phi_b)_k|}\{|\Phi_b|\cos(\beta - \beta_k)\}\cos\omega t \tag{32}$$

The quantity $|(\Phi_b)_k|$ is the magnitude of the largest transverse displacement component of the eigenvector $\{\Phi_b\}$, and β_k is the corresponding phase angle. Next, denote $c = \bar{c}e^{\alpha t}$ as the damped amplitude. Thus, it is clear from Eq. (32) that the sign of the damping rate controls the stability of the solution. When α is equal to zero, $c = \bar{c}$ and the resulting solution corresponds to that of a limit-cycle oscillation. By letting the normalized eigenvector be

$$\{\bar{\Phi}_b\} = \frac{1}{|(\Phi_b)_k|}\{|\Phi_b|\cos(\beta - \beta_k)\} \tag{33}$$

then Eq. (32) becomes

$$\{W_b\}_t = c\{\bar{\Phi}_b\}\cos\omega t \tag{34}$$

In Eq. (34), the dynamic deflection is normalized and scaled to a given limit-cycle amplitude c. The normalized eigenvector $\{\bar{\Phi}_b\}$ is then used to approximate the various element nodal displacements $\{w_b\}_t$ and to evaluate the element nonlinear stiffness matrices. Reassembling to the system level, the nonlinear stiffness matrices, Eqs. (26) and (27), can be written as

$$[K1]_{nl} = c[\overline{K1}]\cos\omega t \tag{35}$$

$$[K2]_{nl} = c^2[\overline{K2}]\cos^2\omega t \tag{36}$$

where the linearized matrices $[\overline{K1}]$ and $[\overline{K2}]$ have the same forms as $[K1]_{nl}$ and $[K2]_{nl}$ given in Eqs. (26) and (27) except they are using the normalized eigenvector $\{\bar{\Phi}_b\}$, Eq. (33), in evaluating the corresponding element matrices.

The homogeneous dynamic equation, Eq. (24), can thus be solved by iteration as a linearized eigenvalue problem of the form

$$\kappa[M_b]\{\Phi_b\} = \left([K]_l + \frac{c\sqrt{2}}{2}[\overline{K1}] + \frac{3c^2}{4}[\overline{K2}]\right)\{\Phi_b\} \tag{37}$$

A more detailed description of the LUM/NTF method is given in Refs. 18 and 31. As for the determination of critical dynamic pressure λ_{cr} in the linear case ($c/h = 0$), the large amplitude ($c/h \neq 0$) limit-cycle dynamic pressure λ_l is determined in the same way when two lowest eigenvalues κ_1 and κ_2 from Eq. (37) coalesce to a value of κ_l.

Results and Discussion

Discrete Kirchhoff Theory Triangular Element

In the selection of a suitable plate element, two factors are considered to be important: accuracy and efficiency. Several elements, including the 24-degree-of-freedom (DOF) rectangular plate and the 54-DOF high-order triangular plate, have been applied to nonlinear panel flutter analyses.[21-23,31] In this study, a 15-DOF triangular element is used for modeling rectangular and triangular panels. The bending displacement vector $\{w_b\}$ has nine DOF: transverse displacement w and the derivatives w_x and w_y at each vertex. The in-plane displacement vector $\{w_m\}$ has six DOF: in-plane displacements u and v at each vertex. The plate-bending element adopted in this study is the discrete Kirchhoff theory (DKT) element.[28-30] Batoz et al.[28] studied the DKT element and concluded that it is one of the most efficient and reliable elements in its class for plates in static bending. In this study, the linear stiffness matrix is based on the work of Refs. 28 and 30, the mass matrix is adopted from Ref. 33, and the aerodynamic and nonlinear stiffness matrices are developed in detail in Ref. 31. The in-plane displacement functions are simply the linear functions in x and y. Rectangular panels are modeled as $3 \times 8 \times 2$ half-plate mesh, and triangular panels are modeled as full-plate mesh as shown in Fig. 1. The dimensions selected for the panels are $a = 12$ in. and $h = 0.050$ in., and the material properties are taken as $E = 10 \times 10^6$ psi, $\nu = 0.3$, $\alpha = 12.5 \times 10^{-6}$ in./in.°F, and $\rho = 0.2588 \times 10^{-3}$ lb-s^2/in^4. The in-plane displacements at the edges are considered to be immovable, i.e., $u(0, y) = u(a, y) = v(x, 0) = v(x, b) = 0$ for rectangular panels.

Temperature Distributions

To study the influence of arbitrary temperature variations on nonlinear flutter response, three temperature distributions for rectangular panels, Fig. 1, have been considered. For nonuniform distributions, maximum temperature is at the center of the panel and minimum at the edges, which act as heat sinks:

Uniform $\quad \Delta T_1 = T_0$

$$\Delta T_2(x, y, z) = \frac{T_0}{4}\left(1 - \cos\frac{2\pi x}{a}\right)\left(1 - \cos\frac{2\pi y}{b}\right)\left(1 + \frac{kz}{h}\right) \tag{38}$$

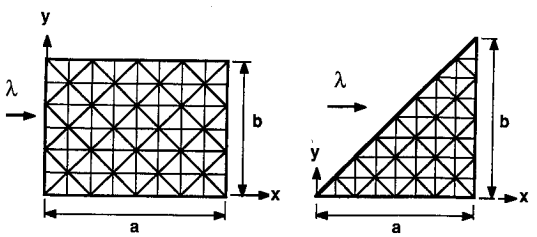

Fig. 1 DKT finite element mesh.

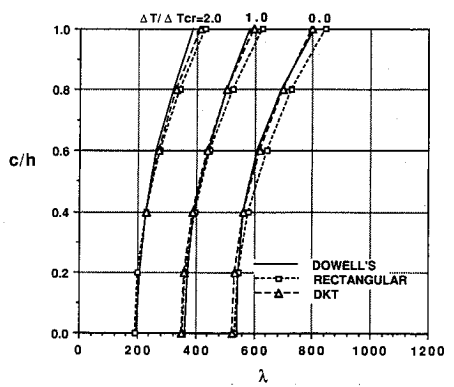

Fig. 2 Comparison of finite element and time integration (six modes) limit-cycle results for a simply supported square panel.

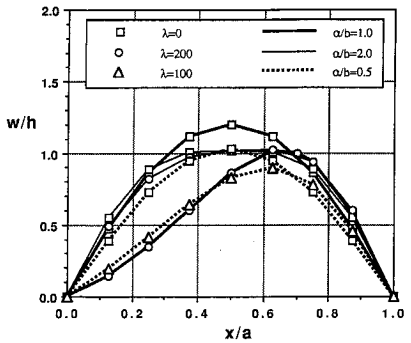

Fig. 3 Deflections of simply supported rectangular panels.

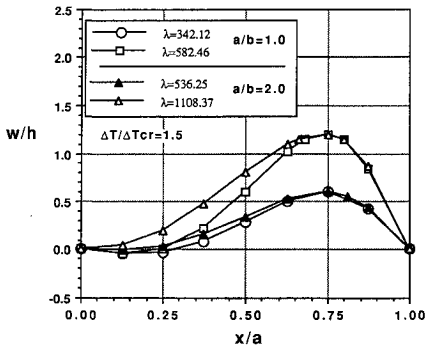

Fig. 4 Limit-cycle deflections of simply supported rectangular panels.

$$\Delta T_3(x, y, z) = T_0 \sin\frac{\pi x}{a}\sin\frac{\pi y}{b}\left(1 + \frac{kz}{h}\right) \tag{39}$$

where $-h/2 \le z \le h/2$, $0 \le k \le 2$, and $k = 0$ corresponds to the fact that there is no temperature gradient through thickness. In the theory of thermoelasticity there are some restrictions on temperature distribution for the exact solutions of plane stress problems. In reality, the temperature could be arbitrary, and the plane stress of Eq. (2) could become an approximation for thin plate.[34]

Comparison with Time Domain Solutions

To demonstrate the accuracy of the present finite element formulation, the classic Galerkin/time integration[9] (using six linear normal modes) and the present finite element (using one updated mode) results are shown in Fig. 2 on the relation of limit-cycle amplitude vs dynamic pressure for a simply supported square panel at several temperature ratios. The relation between the uniform temperature change and the equivalent mechanical force system ($R_x = R_y$ in Ref. 9) is $-R_x/2\pi^2 = \Delta T/\Delta T_{cr}$. Finite element solutions using the 24-DOF rectangular element (3×8 half-plate mesh) are also given. It shows the excellent agreement between the finite element and time domain solutions.

Thermal-Aerodynamic Postbuckling Deflection

It has been known[31] that, before the dynamic pressure reaches its critical value λ_{cr}, a panel buckles due to the combined temperature ($\Delta T/\Delta T_{cr} > 1$) and aerodynamic pressure, whereas beyond λ_{cr} the panel has a limit-cycle oscillation. Figure 3 shows the thermal-aerodynamic postbuckling deflections for simply supported rectangular panels with $a/b = 0.5$, 1.0, and 2.0 at uniform temperature $\Delta T/\Delta T_{cr} = 3.0$ and dynamic pressure $\lambda = 0$, 100, and 200. This figure shows that the panel buckles unsymmetrically due to airflow, and the increase in airflow speed will reduce the buckled deflection and even blow the buckled panel to flat. In addition, the deflection shape is in one half-sine-wave for $a/b = 1.0$ and 2.0 and three half-sine-waves for $a/b = 0.5$ in the width (y) direction.

Limit-Cycle Deflection

The typical panel limit-cycle deflection shapes are shown in Fig. 4 for simply supported square and rectangular ($a/b = 2.0$) panels at uniform temperature $\Delta T/\Delta T_{cr} = 1.5$ and various limit-cycle dynamic pressures. The maximum panel deflections are noted to occur at three-fourths of the panel length. The different limit-cycle amplitudes are excited by corresponding dynamic pressures as shown in Fig. 4.

Maximum Deflection vs Dynamic Pressure

The total panel deflection at $x/a = 0.75$ vs dynamic pressure for a simply supported square panel at various uniform temperatures is shown in Fig. 5. The curves on the left-hand side are the static equilibrium deflections obtained from Eq. (15) for these curves since the λ has not yet reached the critical value; thus the limit-cycle motion has not started ($\{W\}_t = 0$). On the other hand, the curves on the right-hand side are the dynamic limit-cycle amplitudes (c/h) obtained from Eq. (16) or Eq. (24); for these curves the panel has been blown flat ($\{W\}_s = [K1]_{nl} = 0$). The discontinuities of some of the curves for temperature ratio ≥ 2.0 are due to the chaotic region (see Fig. 6).

Map of Panel Behavior

Figure 6 maps the complete behavior of a simply supported square panel under uniform temperature change. In Fig. 6, curve DA is the flutter boundary (λ_{cr} at different temperatures), and the snap-through or chaotic region is bounded by the curve BAE. With the examination of the static equation, Eq. (15), the line CAE divides the flat ($\{W\}_s = 0$) and the buckled ($\{W\}_s \neq 0$) regions. In the region above CAE, Eq. (15) gives a converged trivial solution, $\{W\}_s = 0$, and the panel is flat. In the region below the curve CAB, Eq. (15) gives a converged nontrivial solution, $\{W\}_s \neq 0$; thus the panel is buckled. Within the region of BAE, bifurcation occurs and Eq. (15) fails to yield a converged real solution ($\{W\}_s$ is undetermined). With the examination of the dynamic equation, Eq. (16), it is found that there is no flutter motion in the region below the curve DAB and the panel remains in an equilibrium position. In the region above the curve DAE, Eq. (16) gives a converged limit-cycle solution, the panel oscillates from a flat static equilibrium position ($\{W\}_s = 0$) with a self-sustained harmonic motion. In the region of BAE, Eq. (16) does not give a convergent solution, and also $\{W\}_s$ is undetermined, thus snap-through or chaotic motion happens.[3,4,7,8] The importance of the static equation, Eq. (15), is that it not only deals with the static equilibrium between elastic, thermal, and aerodynamic forces, but also determines the nature of the dynamic solutions due to the coupling of the two equations. The snap-through boundaries can thus be traced out by using the static equation, Eq. (15), alone with increments of temperature and dynamic pressure. In Fig. 6, the curve DA is a critical flutter boundary obtained from Eq. (29) or from Eq. (37) with $c = 0$. With the increase of panel

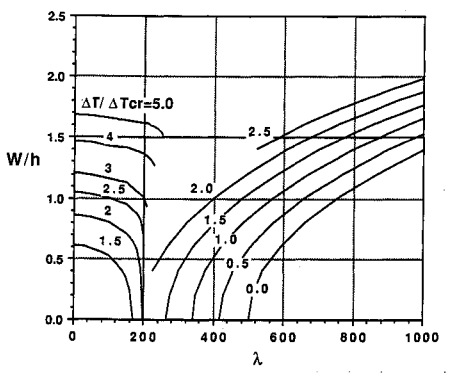

Fig. 5 Maximum deflection vs dynamic pressure for a simply supported square panel with various uniform temperatures.

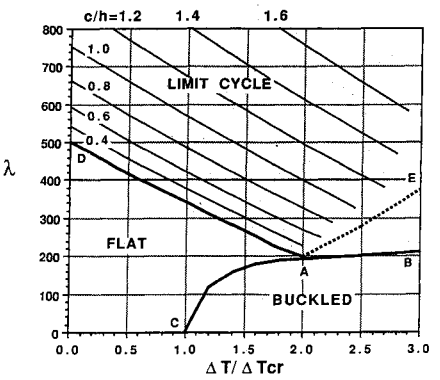

Fig. 6 Stability boundaries and limit-cycle amplitudes of a simply supported square panel with uniform temperature.

flutter amplitude c/h, parallel-like curves can be determined in the limit-cycle region of DAE and the low ends of these parallel curves bound the chaotic motion. Suitable methods such as time integration[8] and amplitude increment[35] are needed to analyze the nonharmonic periodic motions but would increase in computation time. It is also found that, at some combination of moderately large dynamic pressure and temperature, dynamic instability could happen and Eq. (16) will not give a converged solution in the iterative process. This phenomenon was also observed by Dowell in the time domain solution.[7-9]

Influence of Temperature on Flutter Response

Table 1 shows the critical buckling temperature, critical dynamic pressure, limit-cycle dynamic pressure, and thermal-aerodynamic postbuckling deflection for simply supported square and rectangular panels at three temperature distributions ($k = 0$). The following information can be obtained from Table 1:

1) At the same temperature ratio with different distributions, the square panel has less differences in flutter response whereas the rectangular panel has larger differences (but less than 15%).

2) The critical temperatures are important parameters since they are quite different as shown.

3) The thermal stress analysis is essential since an equivalent mechanical load is difficult to be found for complex structures or composite plates.

Effects on Stability Boundaries

Boundary Condition

Figure 7 shows the stability boundaries for simply supported and clamped square panels under uniform temperature distribution. It shows that the more restrained panel is more stable. The minimum critical dynamic pressure, point A in the figure, of the clamped panel is higher than that of the simply supported panel.

Thermal Bending Moment

When there is temperature gradient across the panel thickness, it will produce thermal bending moment in the plate. Figure 8 shows the effects of the thermal bending on the stability boundaries for a simply supported square panel. The curves A1 and A2 correspond to temperature distribution $\Delta T_2(x, y, z)$, Eq. (38), with $k = 1$ and 2, respectively. The curve A0 corresponds to a uniform temperature, which is given for comparison. It can be seen that a higher temperature gradient across the thickness stabilizes the panel and reduces the area of flutter region. Although the flutter region is smaller, the stress lever is higher due to the larger buckled deflection.[31]

Length-to-Width Ratio

In Fig. 9, the stability boundaries are given for simply supported rectangular panels with $a/b = 0.5$, 1.0, and 2.0 under

Table 1 Flutter results of simply supported rectangular panels with different temperature distributions

	T_0	$\frac{T_0}{4}\left(1-\cos\frac{2\pi x}{a}\right)\left(1-\cos\frac{2\pi y}{b}\right)$	$T_0 \sin\frac{\pi x}{a}\sin\frac{\pi y}{b}$
$a/b = 1.0$			
ΔT_{cr}	1.766	5.307	3.549
λ_{cr} (at $\Delta T/\Delta T_{cr} = 0.8$)	371.093	364.632	368.681
λ_{cr} (at $\Delta T/\Delta T_{cr} = 1.2$)	309.117	301.275	307.068
λ_l (at $\Delta T/\Delta T_{cr} = 2.0$, $c/h = 0.4$)	226.500	261.590	225.084
λ_l (at $\Delta T/\Delta T_{cr} = 2.0$, $c/h = 1.0$)	399.093	379.139	390.363
W_s/h (at $\Delta T/\Delta T_{cr} = 3.0$, $\lambda = 100$)[a]	1.145	1.223	1.191
W_s/h (at $\Delta T/\Delta T_{cr} = 3.0$, $\lambda = 180$)[a]	0.967	1.005	0.995
$a/b = 2.0$			
ΔT_{cr}	4.428	12.882	8.755
λ_l (at $\Delta T/\Delta T_{cr} = 1.5$, $c/h = 0.6$)	536.250	557.889	552.750
λ_l (at $\Delta T/\Delta T_{cr} = 1.5$, $c/h = 1.2$)	1108.121	1012.300	1040.625
W_s/h (at $\Delta T/\Delta T_{cr} = 3.0$, $\lambda = 180$)[a]	1.011	1.161	1.106
W_s/h (at $\Delta T/\Delta T_{cr} = 5.0$, $\lambda = 300$)[a]	1.365	1.661	1.557

[a] W_s is at the location of $x = a/2$ and $y = b/2$.

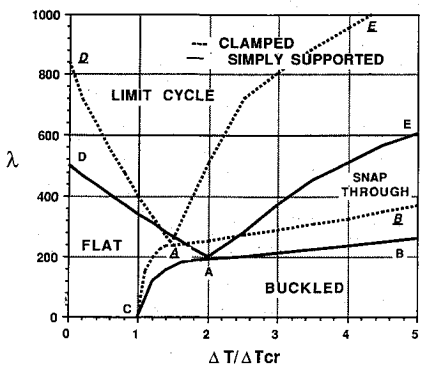

Fig. 7 Stability boundaries of clamped and simply supported square panels with uniform temperature.

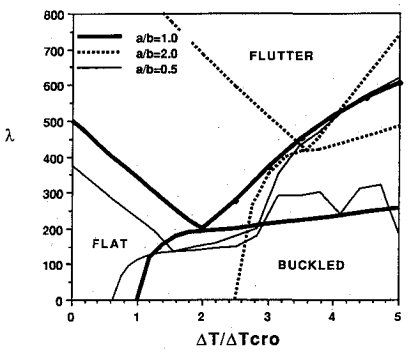

Fig. 9 Stability boundaries of simply supported rectangular panels with uniform temperature.

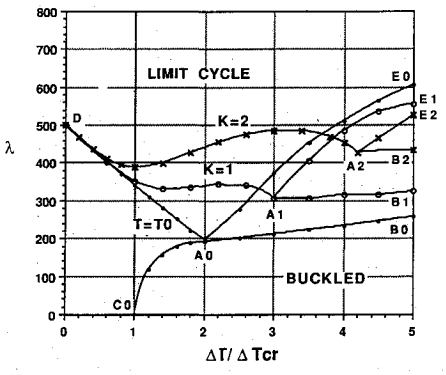

Fig. 8 Stability boundaries of a simply supported square panel with uniform temperature and $\Delta T = (T_0/4)[1-\cos(2\pi x/a)][1-\cos(2\pi y/b)]$ $[1+(kz/h)]$, $k = 1$ and 2.

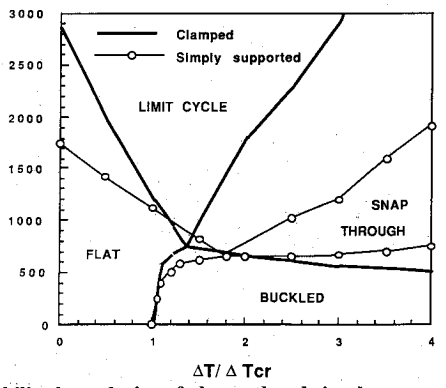

Fig. 10 Stability boundaries of clamped and simply supported triangular panels with uniform temperature.

uniform temperature. The critical buckling temperature is 1.7665°F (ΔT_{cr0}) for the square, 1.1135°F for $a/b = 0.5$, and 4.4284°F for $a/b = 2.0$. The panel of higher length-to-width ratio is much more stable. The curve of $a/b = 0.5$ is strange looking. This is due to the change of its deflection shapes from one half-sine-wave at low temperature to three half-sine-waves at higher temperature in the width (y) direction.

Triangular Panel

Boundary Condition

Figure 10 shows the stability boundaries for simply supported and clamped isoceles triangular panels under uniform temperature. The critical temperature and dynamic pressure are 4.44°F and 1751 for the simply supported and 12.79°F and 2869 for the clamped triangular panel, respectively. The clamped triangular panel is certainly more stable than the simply supported triangular panel, and both are much more stable than the square panels.

Reversed Direction of Airflow

If a surface consists of triangular panels, the airflow could affect panels in two ways. Figure 11 shows the limit-cycle response for a triangular plate under an airflow with reversed direction. The linear dynamic pressure λ_{cr} and flutter frequencies for these two cases are the same, although their flutter modes are different. The limit-cycle dynamic pressures λ_l are different upon the effects of large amplitudes ($c/h \neq 0$).

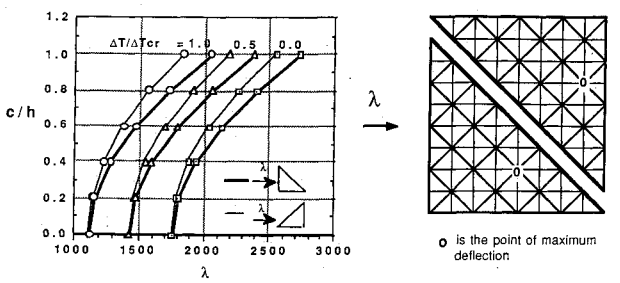

Fig. 11 Limit-cycle response of a simply supported triangular panel with uniform temperature under reversed airflow.

Conclusions

A consistent and unique formulation and an innovative solution procedure are presented for finite element analysis of nonlinear panel flutter with effects of temperature. A panel under different combinations of thermal and aerodynamic loads can have various behaviors: flat, buckled, limit-cycle vibration, and chaotic motion. This solution procedure indicates that the static equilibrium of the panel is acquired from the particular solution and the flutter dynamic response is obtained from the homogeneous solution of the differential equation of motion of the panel. The finite element differential equations of motion consist of a time-independent thermal load vector. The system equation of motion is thus separated into two sets of equations, static and dynamic, which are coupled and have to be solved sequentially. Using the Newton-Raphson iteration, the static equation gives the thermal-aerodynamic equilibrium position, and with application of the LUM/NTF approximation method, the dynamics equation yields the limit-cycle oscillations. The static equilibrium solution plays a significant role in panel stability, and it also influences the characteristics of the dynamic motion. A flat equilibrium position of the panel leads to a harmonic limit-cycle motion, and a thermal-aerodynamically buckled panel would have nonharmonic periodic response or snap-through chaotic motion.

In general, the thermal stress analysis is necessary for nonlinear panel flutter. The temperature gradient across the panel thickness, the larger length-to-width ratio, and the more restrained boundary support condition will all produce more stable flutter response.

The DKT triangular element adopted in this study has proved that this element is accurate and efficient for nonlinear thermal structural and flutter analyses.

Acknowledgment

This work was supported by NASA Langley Research Center under the Master Contract Agreement NAS1-18584, Task Authorization 38, entitled "Thermal Effects on Nonlinear Panel Flutter."

References

[1]Cunningham, H. J., "Flutter Analysis of Flat Rectangular Panels Based on Three-Dimensional Supersonic Unsteady Potential Flow," NASA TRR-256, Feb. 1967.

[2]Dugundji, J., "Theorerical Considerations of Panel Flutter at High Supersonic Mach Numbers," *AIAA Journal,* Vol. 4, No. 7, 1966, pp. 1257–1266.

[3]Xue, D. Y., and Mei, C., "Finite Element Nonlinear Flutter and Fatigue Life of Two-Dimensional Panels with Temperature Effects," *Proceedings of the AIAA/ASME/ASCE/AHS/ASC 32nd Structures, Structural Dynamics, and Materials Conference* (Baltimore, MD), AIAA, Washington, DC, April 1991, pp. 1981–1991.

[4]Dowell, E. H., "Panel Flutter: A Review of the Aeroelastic Stability of Plates and Shells," *AIAA Journal,* Vol. 8, No. 3, 1970, pp. 385–399.

[5]Reed, W. H., Hanson, P. W., and Alford, W. J., "Assessment of Flutter Model Testing Relating to the National Aero-Space Plane," NASA CN-156,823, July 1987.

[6]Ashley, H., and Zartarian, G., "Piston Theory—A New Aerodynamic Tool for the Aeroelastician," *Journal of the Aeronautical Sciences,* Vol. 23, No. 12, 1956, pp. 1109–1118.

[7]Ventres, C. S., and Dowell, E. H., "Comparison of Theory and Experiment for Nonlinear Flutter of Loaded Plates," *AIAA Journal,* Vol. 8, No. 11, 1970, pp. 2022–2030.

[8]Dowell, E. H., "Nonlinear Oscillations of a Fluttering Plate II," *AIAA Journal,* Vol. 5, No. 10, 1967, pp. 1856–1862.

[9]Dowell, E. H., "Nonlinear Oscillations of a Fluttering Plate," *AIAA Journal,* Vol. 4, No. 7, 1966, pp. 1267–1275.

[10]Eslami, H., "Nonlinear Flutter and Forced Oscillations of Rectangular Symmetric Cross-Ply and Orthotropic Panels Using Harmonic Balance and Perturbation Method," Ph.D. Dissertation, Department of Mechanical Engineering and Mechanics, Old Dominion Univ., Norfolk, VA, 1987.

[11]Eastep, F. E., and McIntosh, S. C., "Analysis of Nonlinear Panel Flutter and Response Under Random Excitation or Nonlinear Aerodynamic Loading," *AIAA Journal,* Vol. 9, No. 3, 1971, pp. 411–418.

[12]Kuo, C. C., Morino, L., and Dugundji, J., "Perturbation and Harmonic Balance Methods for Nonlinear Panel Flutter," *AIAA Journal,* Vol. 10, No. 11, 1972, pp. 1479–1484.

[13]Morino, L., "A Perturbation Method for Treating Nonlinear Panel Flutter Problems," *AIAA Journal,* Vol. 7, No. 3, 1969, pp. 405–410.

[14]Olson, M. D., "Some Flutter Solutions Using Finite Element," *AIAA Journal,* Vol. 8, No. 4, 1970, pp. 747–752.

[15]Mei, C., "A Finite Element Approach for Nonlinear Panel Flutter," *AIAA Journal,* Vol. 15, No. 8, 1977, pp. 1107–1110.

[16]Rao, K. S., and Rao, G. V., "Large Amplitude Supersonic Flutter of Panels with Ends Elastically Restrained Against Rotation," *Computers and Structures,* Vol. 11, No. 3, 1980, pp. 197–201.

[17]Sarma, B. S., and Varadan, T. K., "Nonlinear Panel Flutter by Finite Element Method," *AIAA Journal,* Vol. 26, No. 5, 1988, pp. 566–574.

[18]Gray, C. E., Jr., Mei, C., and Shore, C. P., "Finite Element Method for Large Amplitude Two-Dimensional Panel Flutter at Hypersonic Speeds," *AIAA Journal,* Vol. 29, No. 2, 1991, pp. 290–298.

[19]Mei, C., and Weidman, D. J., "Nonlinear Panel Flutter—A Finite Element Approach," *Computational Methods for Fluid-Structure Interaction Problems,* edited by T. Belytschko, and T. L. Geers, AMDVol. 26, American Society of Mechanical Engineers, New York, Nov. 1977, pp. 139–165.

[20]Mei, C., and Wang, H. C., "Finite Element Analysis of Large Amplitude Supersonic Flutter of Panels," *Proceedings of the International Conference on Finite Element Methods* (Shanghai, China), Gordon & Breach, New York, Aug. 1982, pp. 944–951.

[21]Han, A. D., and Yang, T. Y., "Nonlinear Panel Flutter Using High-Order Triangular Finite Elements," *AIAA Journal,* Vol. 21, No. 10, 1983, pp. 1453–1461.

[22]Dixon, I. R., and Mei, C., "Finite Element Analysis of Nonlinear Flutter of Composite Panels," *Proceedings of the AIAA/ASME/ASCE/AHS/ASC 32nd Structures, Structural Dynamics, and Materials Conference* (Baltimore, MD), AIAA, Washington, DC, April 1991, pp. 2002–2010.

[23]Liaw, D. G., and Yang, T. Y., "Nonlinear Supersonic Flutter and Reliability of Uncertain Laminated Plates," *Proceedings of the AIAA/ASME/ASCE/AHS/ASC 32nd Structures, Structural Dynamics, and Materials Conference* (Baltimore, MD), AIAA, Washington, DC, April 1991, pp. 1964–1970.

[24]Houbolt, J. D., "A Study of Several Aerothermoelastic Problems of Aircraft Structure in High-Speed Flight," Ph.D. Thesis, Institut für Flugzeugstatik und Leichtbau, Swiss Federal Inst. of Technology, Zurich, Switzerland, 1958.

[25]Schaeffer, H. G., and Heard, W. L., Jr., "Flutter of a Flat Plate Exposed to a Nonlinear Temperature Distribution," *AIAA Journal,* Vol. 3, No. 10, 1965, pp. 1918–1923.

[26]Yang, T. Y., and Han, A. D., "Flutter of Thermally Buckled Finite Element Panels," *AIAA Journal,* Vol. 14, No. 7, 1976, pp. 975–977.

[27]Xue, D. Y., Mei, C., and Shore, C. P., "Finite Element Two-Dimensional Panel Flutter at High Supersonic Speeds and Elevated Temperature," *Proceedings of the AIAA/ASME/ASCE/AHS/ASC 31st Structures, Structural Dynamics, and Materials Conference* (Long Beach, CA), AIAA, Washington, DC, April 1990, pp. 1464–1475.

[28]Batoz, J. L., Bathe, K. J., and Ho, L. W., "A Study of Three-Node Triangular Plate Bending Elements," *International Journal for Numerical Methods in Engineering,* Vol. 15, No. 12, 1980, pp. 1771–1812.

[29]Hughes, T., Taylor, R., and Kanoknukulchai, W., "A Simple and Efficient Finite Element for Plate Bending," *International Journal for Numerical Methods in Engineering,* Vol. 11, No. 10, 1977, pp.

1529–1543.
[30]Jeyachadrabose, C., and Kirkhope, J., "An Alternative Explicit Formulation for the DKT Plate—Bending Element," *International Journal for Numerical Methods in Engineering,* Vol. 21, No. 7, 1985, pp. 1289–1293.
[31]Xue, D. Y., "Finite Element Frequency Domain Solution of Nonlinear Panel Flutter with Temperature Effects and Fatigue Life Analysis," Ph.D. Dissertation, Department of Mechanical Engineering and Mechanics, Old Dominion Univ., Norfolk, VA, 1991.
[32]Chiang, C. K., Mei, C., and Gray, C. E., Jr., "Finite Element Large-Amplitude Free and Forced Vibrations of Rectangular Thin Composite Plates," *ASME Journal of Vibration and Acoustics,* Vol. 113, July 1991, pp. 309–315.
[33]Zienkiewicz, O. C., *The Finite Element Method,* 3rd ed., McGraw-Hill, London, England, UK, 1971, p. 187.
[34]Boley, B. A., and Weiner, J. H., *Theory of Thermal Stresses,* Robert E. Krieger Publishing Co., Malabar, FL, 1985, p. 406.
[35]Lau, S. L., and Cheung, Y. K., "Amplitude Incremental Variational Principle for Nonlinear Vibration of Elastic Systems," *ASME Journal of Applied Mechanics,* Vol. 48, Dec. 1981, pp. 959–964.